Crystallization and Melting Behavior of the Crystalline Soft Segment in a Shape-Memory Polyurethane Ionomer

Yong Zhu,[1] Jinlian Hu,[1] Ka-Fai Choi,[1] Kwok-Wing Yeung,[2] Qinghao Meng,[1] Shaojun Chen[1]

[1]*Institute of Textiles and Clothing, Hong Kong Polytechnic University, Kowloon, Hong Kong, People's Republic of China*
[2]*Clothing Industry Training Authority, Kowloon, Hong Kong, People's Republic of China*

Received 28 December 2006; accepted 4 June 2007
DOI 10.1002/app.26969
Published online 24 September 2007 in Wiley InterScience (www.interscience.wiley.com).

ABSTRACT: To illustrate the crystallization properties of soft segments in shape-memory polyurethane (SMPU) ionomers, a series of SMPU ionomers with various ionic group contents and two kinds of counterions were synthesized with a prepolymerization method. An isothermal crystallization kinetic method was used to analyze the effects of ionic groups within the hard segments on the crystallization of the soft segments in a heating and cooling routine similar to that in a shape-memory function. The more ionic groups there were within the hard segments, the lower the crystallization rate was of the soft segments. The crystallization mechanism of the SMPU ionomers was quite close to that of a control sample on the basis of similar Avrami exponents; the counterion category also had some influence on the crystallization rate. Meanwhile, the melting behavior after isothermal crystallization reflected the fact that the thermal history of the hard segments had a huge effect on the crystallization mechanism of the soft segments. Especially for the SMPU ionomer quenched from 240°C, the crystallization time dependence of the secondary crystallization was rather significant, but for the SMPU ionomer quenched from 70°C, the primary crystallization of the poly(ε-caprolactone) soft segment was predominant. © 2007 Wiley Periodicals, Inc. J Appl Polym Sci 107: 599–609, 2008

Key words: crystallization; ionomers; polyurethanes

INTRODUCTION

Segmented shape-memory polyurethanes (SMPUs) are thermoplastic block copolymers with unique mechanical properties due to the thermoresponsive shape-memory effect. Because of the presence of soft and hard segments, the former comprising the reversible phase and the latter forming the frozen phase, the original shape of the materials can be restored when they are heated above a certain temperature after being strained. This unique feature has made this type of material attract serious research interest from both academia and industry in the past 2 decades.[1–19] Li and coworkers[3,20,21] investigated the relations between the shape-memory effect and the molecular structure of segmented polyurethane (PU) with poly(ε-caprolactone) (PCL) as the soft segment.[3,20,21] The authors concluded that the high crystallinity of the soft-segment regions at room temperature was a prerequisite for the segmented copolymers to demonstrate shape-memory behavior. Accordingly, a lower limit of the PCL molecular weight (~2000–3000), below which the PCL segments were not able to crystallize under the usual processing conditions, was then established. The immediate conclusion is that crystallization plays an important role in shape fixation in segmented PU. In addition, it was observed by Bogdanow et al.[22] that the crystallinity, crystallization rate, and physical mobility of the PCL soft segment during crystallization depend on the hard-segment content, the length of the soft segment, and the total molecular weight of the block copolymer [poly(ether urethane)s (PEUs) in their case]. Taking into account these interrelated parameters, the authors concluded that (1) crystallization was inhibited by the shortening of the crystallizable block resulting from the enhanced number of interconnections between the soft and hard segments and (2) the crystallizability of the PEUs was inversely proportional to the total molecular weight of the polymer: the highest degree of crystallinity could be achieved with the lowest molecular weight PEUs. Therefore, it can be concluded that the soft-segment length, hard-segment content, and total molecular weight play important roles in the crystallization of the crystallizable soft phase in segmented PU.

In recent years, numerous studies on PU ionomers have emerged because of their superior mechanical and thermal properties. For example, the tensile strength, modulus, and elongation at fracture of PU ionomers in the form of thin films can be increased

Correspondence to: J. Hu (tchujl@inet.polyu.edu.hk).
Contract grant sponsor: Hong Kong Innovation and Technology Fund (ITF); contract grant number: ITS 098/02.

TABLE I
Formulation of the SMPU Ionomers

Sample	PCL (wt %)	BIN (wt %)	PCL (mol)	BIN (mol)	BDO (mol)	MDI (mol)	HAc (mol)	C8I (mol)
75-0	75	0	1	0	9.07	10.07	0	0
BIN75-6	75	6	1	3.81	3.91	8.71	3.81	0
BIN75-11	75	10.56	1	6.7	0	7.7	6.7	0
BIN75-6-C8	75	6	1	3.81	3.91	8.71	0	3.81
BIN75-11-C8	75	10.56	1	6.7	0	7.7	0	6.7

because of the presence of Coulombic forces between the ionic centers within the polymer backbone.[7,23,24] Kim et al.[7] demonstrated the existence of a shape-memory effect in segmented PU ionomers based on PCL with various structural parameters, such as the soft-segment length, hard-segment content, and ionic groups.[7] Their differential scanning calorimetry (DSC) results indicated that for PCL [weight-average molecular weight (M_w) = 4000]-based PUs with a 70% soft-segment content, the PU nonionomers and ionomers showed similar thermal behavior, except that the nonionomers had a slightly lower heat of crystallization and heat of fusion, which implied an enhancement of the microphase separation in the ionomers. However, when the soft-segment content was 55% and the soft-segment length was the same, its crystallization was observed solely in nonionomers and not in ionomers. Accordingly, it is concluded that a twofold effect of ionic groups within hard segments exists and that the molecule has a different physical structure. As a result, the microphase separation has different morphologies, leading to diverse soft-segment crystallization, which greatly affects the shape-memory property. In general, the effects of ionic groups on the crystallization of the soft segment cannot be ignored, especially for segmented PU. This effect can thus be used as design guidance for novel segmented PU ionomers having unique physical properties.

As previously report, the introduction of ionic groups into the hard segment is expected to cause a segmented PU ionomer to possess some novel functions, such as antibacterial activity,[25] ionic conductivity,[26] high tensile modulus and tensile strength at room temperature,[7] and increased water vapor permeability.[24] To understand the role played by ionic groups within the hard segment on the shape-memory function, the first step is to elucidate the effects of ionic groups within the hard segment on the crystallization of the soft segment. To assess the effectiveness of the shape-memory effect in practice, the copolymers are subjected to a testing routine including the heating, deforming, and cooling of samples. The testing cycle calls for a through understanding not only of the crystallinity and melting temperature (T_m) of crystallization but also of the crystallization rate and crystallizability. In this study, a series of PCL-based segmented SMPU ionomers with various ionic group contents and counterions were synthesized. The effects of different ionic group contents and counterions on the crystallizability and melting behavior were studied with isothermal crystallization kinetics. Two parameters in the Avrami equation depending on the nucleation details, n [the Avrami (Ozawa) exponent, the value of which depends on the mechanism of nucleation and the crystal-growth geometry] and K (a rate constant containing the nucleation and growth parameters), were determined for SMPU ionomers.

EXPERIMENTAL

Sample preparation

SMPU ionomers were synthesized from PCL diols, 4,4′-diphenylmethane diisocyanate (MDI), 1,4-butanediol (BDO), and *N,N*-bis(2-hydroxyethyl)isonicotinamide (BIN). The formulation of the PU samples is shown in Table I. PCL diols (Daicel Chemical Industries, Ltd., Tokyo, Japan) with $M_w \sim 10{,}000$ were dried and degassed at 80°C under 1–2 mmHg for 24 h for PU synthesis. Extra-pure-grade MDI (Kasei Kogyo Co, Ltd., Tokyo, Japan), BDO, and BIN (Sigma-Aldrich Chemical Co., St. Louis, MO) were used to synthesize the SMPU ionomer samples. Acetic acid (HAc; International Laboratory, San Bruno, CA) and 1-iodooctane (C8I; International Laboratory) were used to neutralize BIN with the same number of moles.[27,28] Dimethylformamide (DMF) (Ajax Finechem Ltd., Auckland, New Zealand) was dehydrated with 4-Å molecular sieves for several days in advance before its use as a solvent in PU synthesis. The SMPU ionomer samples were then placed in a dry nitrogen atmosphere before use.

The reaction to prepare the prepolymer with PCL and MDI was carried out at 80°C for 2 h in a 500-mL, round-bottom, four-necked flask filled with nitrogen and equipped with a mechanical stirrer, a thermal meter, and a condenser. Following the chain-extension process with BDO and/or BIN for another 2 h, the neutralization reaction was carried out at 65°C for 2 h through the subsequent addition

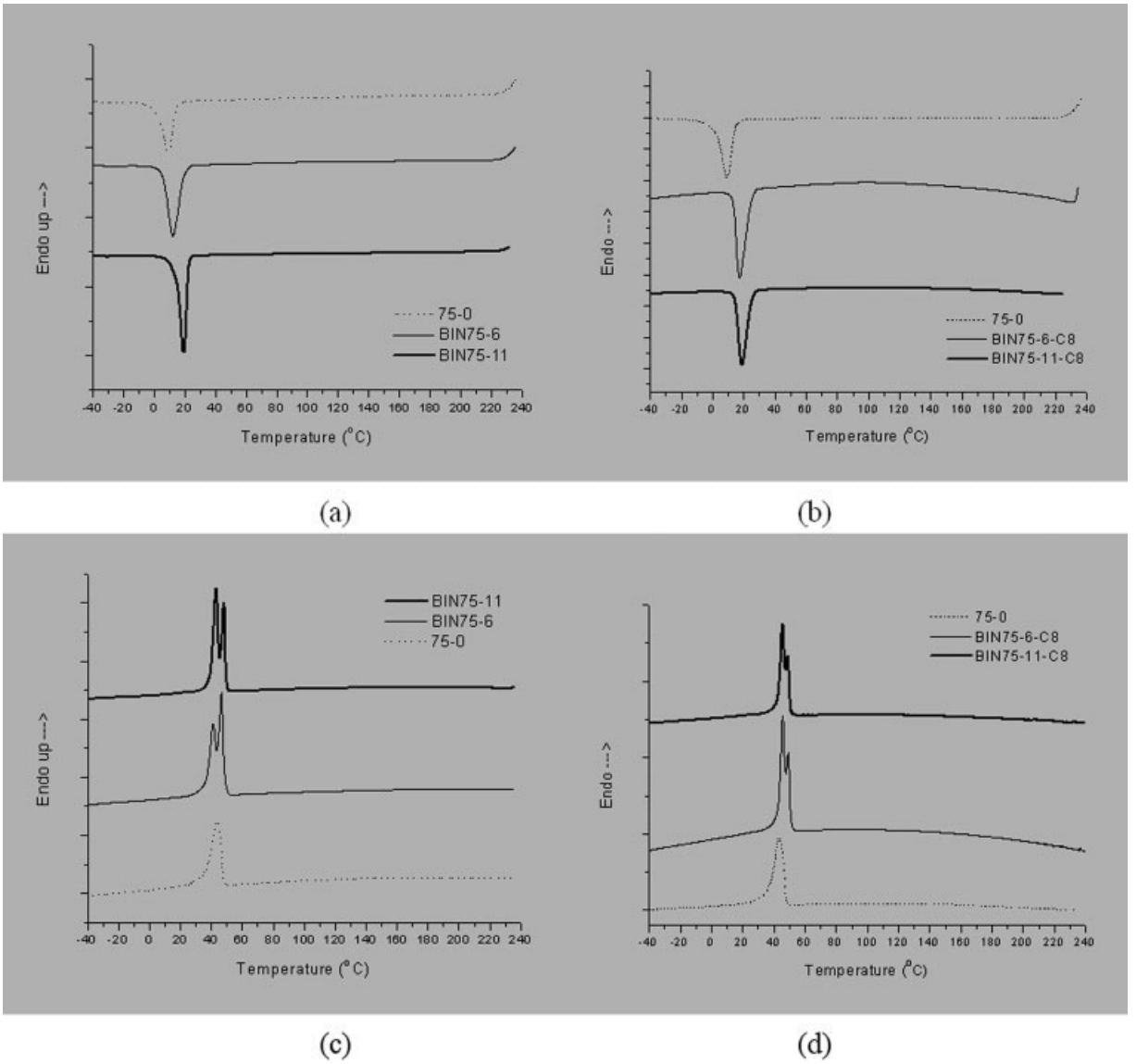

Figure 1 DSC (a,b) cooling and (c,d) heating scans for the SMPU ionomers.

of a stoichiometric amount of the HAc or C8I agent.[27,28] SMPU ionomer films were prepared through the transfer of some of the PU solution to Teflon molds and allowed to solidify at 60°C in air for 24 h. To remove the residual DMF, the films were held at 75°C under a vacuum of 1–2 mmHg for 24 h subsequently. The nominal thickness of the films was about 100 μm.

In this study, we fixed the soft-segment content and length in the SMPU ionomers to investigate the effect of the ionic group content on the crystallization of PCL (number-average molecular weight = 10,000)-based SMPU. The series of SMPU ionomers neutralized with HAc are named by the abbreviation of the ion chain extender followed by 3 numbers, as shown in Figure 1. The first two numbers denote the soft-segment content, and the third number represents the BIN weight. For example, sample BIN75-11 contained 75 wt % soft segment, approximately 11 wt % BIN, and the default neutralization agent HAc. Sample 75-0 contained no BIN but only MDI, BDO, and PCL (number-average molecular weight = 10,000) and was used as the control sample in this study. The samples neutralized with C8I are named similarly to those neutralized with HAc; for instance, for BIN75-11-C8, ''-C8'' illustrates that the neutralization agent was C8I.

DSC measurements

The thermal properties of the PU samples were investigated with DSC (Diamond, PerkinElmer, Waltham, MA), purged with nitrogen gas, and cooled with a cooler (Intracooler II, PerkinElmer). Indium

and zinc standards were used for calibration. To ensure a consistent thermal history for the melting process, the samples were heated to 240°C and kept there for 3 min. After that, they were cooled to −100°C at a cooling rate of 10°C/min and then heated to 240°C at a rate of 10°C/min, and the thermograms were recorded and compared.

Isothermal crystallization

Isothermal crystallization experiments were performed with a PerkinElmer Diamond differential scanning calorimeter, and the heating and cooling routine and isothermal crystallization temperature (T_c) were quite similar to those used in a shape-memory function investigation.[29] The sample (~4–6 mg) was initially heated to 70°C at a rate of 10°C/min and held there at 70°C for 5 min to remove the thermal history of the crystallizable phase; then, it was rapidly (60°C/min) cooled to a designated T_c, and it was held at this temperature to the end of the exothermic crystallization. The heat of fusion during the isothermal crystallization process was recorded as a function of time. T_c was chosen from a practical range of 16–28°C.

The amounts of heat generated during the development of the crystal phase were recorded and analyzed according to the usual equation used for evaluating the relative degree of crystallinity (X_t):

$$X_t = \frac{\int_{t_0}^{t} (\frac{dH}{dt}) dt}{\int_{t_0}^{t=\infty} (\frac{dH}{dt}) dt} \quad (1)$$

where t_0 and $t = \infty$ are the time at which the sample reaches isothermal conditions (as indicated by a flat baseline after an initial spike in the thermal curve) and the time at which the dominant sharp exothermic peak ends, respectively. H is the enthalpy of crystallization at time t. After isothermal crystallization, the sample was heated to 100°C, and T_m, indicated by the maximum of the endothermic peak, was recorded.

RESULTS AND DISCUSSION

DSC measurements

The thermograms of all the studied SMPU ionomers showed the exothermic crystallization peak of the soft segments in the cooling scan and the endothermic melting peak of the soft segments in the reheating (second heating) scan, as shown in Figure 1. The crystallization and melting behaviors of the hard segments could not be detected in this testing cycle. Brunette et al.[30] studied a model hard-segment compound, BDO-MDI, with DSC and Fourier transform infrared spectroscopy, which revealed the temperature dependence of hydrogen bonding, and they concluded that sufficient annealing at 150°C could effectively convert the noncrystalline domain structure into the crystalline state, which gave rise to a well-defined high-temperature transition at 200–230°C.[30] For the hard segment MDI-BDO in PCL-based segmented PU, Li et al.[31] reported that the melting peak of the hard segment in a DSC heating scan could not be detected in film-cast specimens with a hard-segment content of 7.77–18.7 wt % and a soft-segment length of 7000.[31] However, the endothermic peaks appeared in DSC thermographs for a specimen with an 18.7 wt % hard-segment content after an annealing treatment. Bogart et al.[32] investigated compression-molded PU samples composed of MDI, BDO, and PCL (number-average molecular weight = 2000) with DSC. In a DSC heating scan, they found that the endothermic peaks of the hard segments began to be detected when the hard-segment content was 45 wt % or greater, and an increase in the hard-segment content increased the size and peak position temperature of the hard-segment melting endotherm; this was due to the fact that longer hard segments produced better phase-separated systems that were more readily crystallizable.[32] Therefore, in our DSC testing, the absence of melting peaks of hard segments should have been caused by the relatively low hard-segment content, insufficient annealing time, and relatively low annealing temperature during the film-casting procedures. The thermal property data are shown in detail in Table II. The T_c value of the soft segments in the cooling scan increased significantly with increasing ionic group content, and the enthalpies of crystallization of the soft segments in the four SMPU ionomer specimens were quite similar but higher than that of the control sample (75-0). Generally, the enthalpy of crystallization in a cooling scan can be used to investigate the crystallizability of a specimen. Therefore, the resultant data from the cooling scan suggest that the soft segments of SMPU ionomers have stronger crystallizability. Accordingly, it can be observed that, in the reheating scan, the melting point of the soft segments and the melting enthalpy of the soft segments of these two series of SMPU ionomers (neutralization by HAc or C8I) were higher than those of 75-0. The crystallinity of the segmented PU ionomer samples was calculated from the enthalpy of 100% crystalline PCL (32.4 cal/g) given by Crescenzi et al.[33] Therefore, it could be concluded that, in comparison with the control sample, the crystallinity of the soft segment in segmented PU was significantly raised with the existence of ionic groups within the hard segment. According to the mechanism of the shape-memory effect proposed for segmented copolymers in previous studies,[3,9,21] the crystalline

TABLE II
Thermal Properties of the SMPU Ionomers

	First heating at 10°C/min			Second heating at 10°C/min			Cooling at 10°C/min	
Sample	T_{ms} (°C)	δH_{ms} (J/g)	Crystallinity (%)	T_{ms} (°C)	δH_{ms} (J/g)	Crystallinity (%)	T_{cs} (°C)	δH_{cs} (J/g)
75-0	49.20	39.37	38.6	43.46	35.62	34.9	9.17	32.33
BIN75-6	46.94	39.81	39.0	46.63 (41.09)	50.60	49.6	12.14	44.87
BIN75-11	47.46	41.75	40.9	48.50 (43.29)	49.45	48.5	19.59	43.97
BIN75-6-C8	53.05	52.67	51.61	45.51 (49.21)	46.12	45.19	17.27	44.50
BIN75-11-C8	53.21	52.75	51.69	45.68 (49.03)	42.07	41.22	18.91	41.48

δH_{cs} = enthalpy of crystallization of soft segments; δH_{ms} = melting enthalpy of soft segments; T_{cs} = crystallization temperature of soft segments; T_{ms} = melting point of soft segments.

soft segment is responsible for the fixity of deformation. Therefore, it is expected that higher crystallinity of the soft segment will facilitate temporary deformation fixity and subsequently improve the fixity ratio. Besides, there are dual-melting features in all the DSC reheating thermograms shown in Figure 1. A similar signature was also observed for a 30/70 diglycidyl ether of bisphenol A/PCL blend,[34] binary blends of solution-chlorinated polyethylenes with PCL, blends of poly (hydroxyl ether of bisphenol A) (phenoxy) with PCL,[35,36] and PCL/poly(styrene-co-acrylonitrile)(SAN).[37] In a study of phenoxy/PCL by Defieuw et al.,[36] the isothermal crystallization process was interrupted after different times, and the DSC melting trace was immediately recorded. The higher melting endotherm was at a fixed temperature after short isothermal crystallization times (primary crystallization), whereas the lower melting peak appeared only after much longer crystallization times (secondary crystallization). The secondary crystallization was supposed to occur in the amorphous phase segregated during the primary crystallization of PCL, resulting in a slower crystallization process as this happened in the presence of a higher phenoxy concentration. In our study, a similar routine was used to investigate the dual-melting behavior of SMPU ionomers. To remove the effect of recrystallization in the cooling process, a sample was quenched to T_c from 70°C with a high enough cooling rate (60°C/min). The T_c value was 20°C, as shown in Figure 2. In the previously applied routine, the high temperature, 70°C, and the low temperature, 20°C, corresponded to the deforming temperature and fixing temperature of the shape-memory function cycle, respectively, as reported previously by our group.[29] Just like the results in the investigation of phenoxy/PCL blends studied by Defieuw et al., Figure 2 shows that the highest melting endotherm resided in a constant area and position from 45 to 50°C in the heating scan after isothermal crystallization for various times; however, the lower melting endotherm kept moving upward with an increase in the isothermal crystallization time from 0.5 to 120 min. After isothermal crystallization at T_c = 20°C, the main melting peak area was from the primary crystallization, and this was not as obvious as the dual-melting peak behavior in the heating scan after cooling at 10°C/min from 240°C, as shown in Figure 1. Therefore, this investigation was repeated for sample BIN75-11 under a different thermal history as follows: (1) isothermal crystallization at 20°C after quenching from 75°C, (2) isothermal crystallization at 20°C after quenching from 120°C, and (3) isothermal crystallization at 20°C after quenching from 240°C. The results presented in Figure 3 suggest that the specimen quenched from 240°C showed a significant dual-melting peak after isothermal crystallization for a short time such as 5 min, but for a longer time, a single melting peak appeared that might be from the two overlapping peaks. For the samples quenched from 75 and 120°C, the primary crystallization was still predominant after various isothermal crystallization times. In addition, as shown in Table II, the highest crystallinity of the PCL soft segments was observed for the film-cast specimens neutralized with C8I, such as BIN75-11-C8. Instead, in the second heating scan, the highest crystallinity of the PCL soft segments appeared in specimens neutralized with HAc, such as BIN75-6. Just as previously described, the distinct dual-melting peaks, related to the secondary crystallization, appeared only for the sample quenched from 240°C. For the samples in the first heating scan, the thermal history was film casting at 65 and 70°C for 24 h and cooling at room temperature. However, in the second heating scan, the samples were all treated with heating up to 240°C to remove the previous thermal history and then with cooling at 10°C/min to −100°C, and they accordingly showed obvious dual-melting peaks. Therefore, the thermal history and neutralization agent both had a significant influence on the crystallization of the PCL soft segments in these two series of SMPU ionomers.

Analysis of the isothermal crystallization kinetics

The overall kinetics of the isothermal crystallization of crystalline soft segments from a melt can be ana-

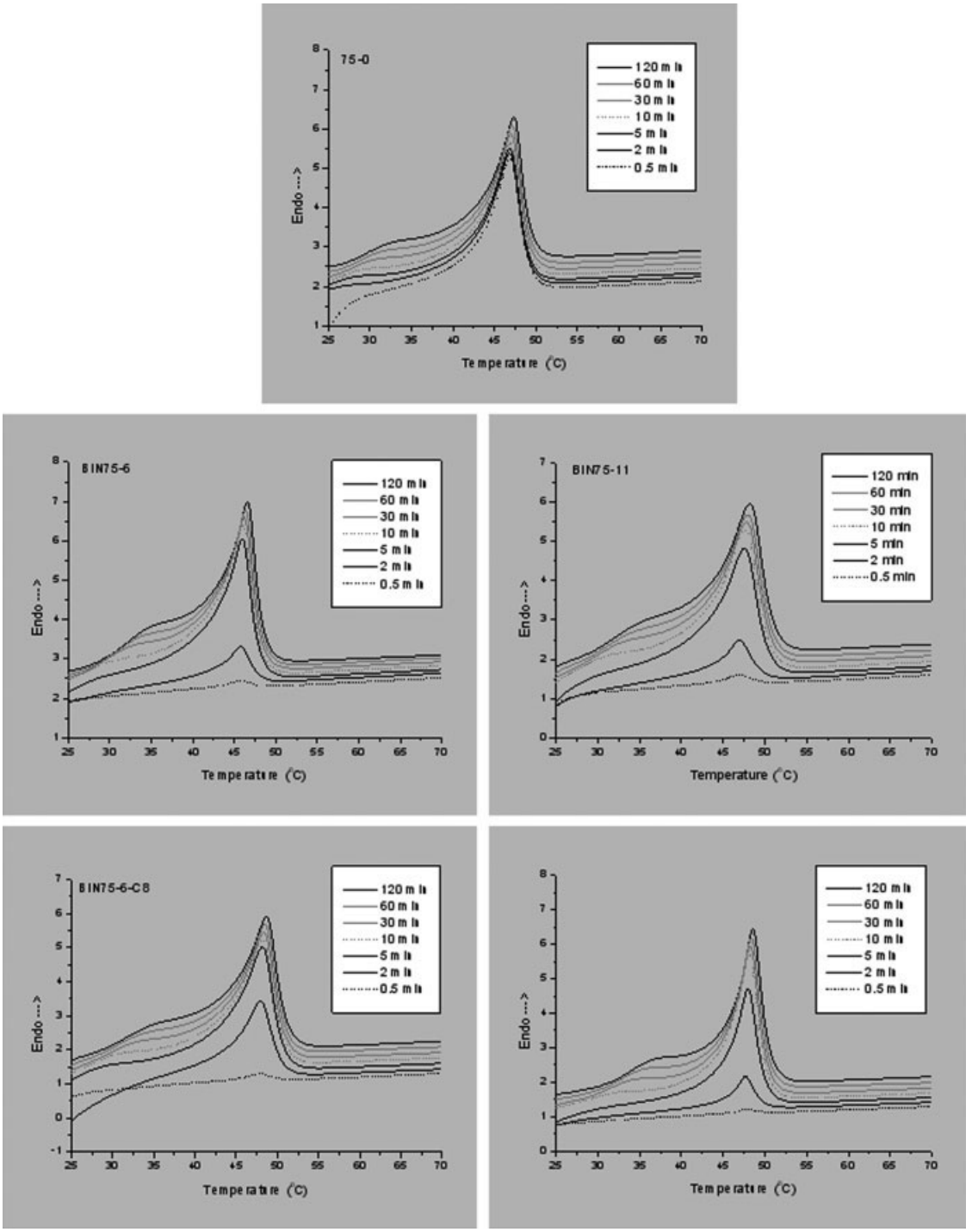

Figure 2 Heating scan after isothermal crystallization at 20°C for various times.

lyzed on the basis of the Avrami equation.[38] This crystallization theory is widely accepted to describe the physical behavior of a variety of crystallization processes, such as semicrystallization in polymers, polymer blends, and copolymers.[39–44] We use a modified Avrami equation called the Ozawa equation to describe the crystallization kinetics:

$$X(t) = 1 - \exp(-Kt^n) \tag{2}$$

This can be linearized into the following form:

$$\log[-\ln(1 - Xt))] = n \log t + \log K \tag{3}$$

where $X(t)$ represents the relative amount of crystallization, which is plotted in Figure 4 for different T_c values and in Figure 5 for SMPU ionomers with various ionic group contents at 28°C. Therefore, if the crystallization rate is compared according to the

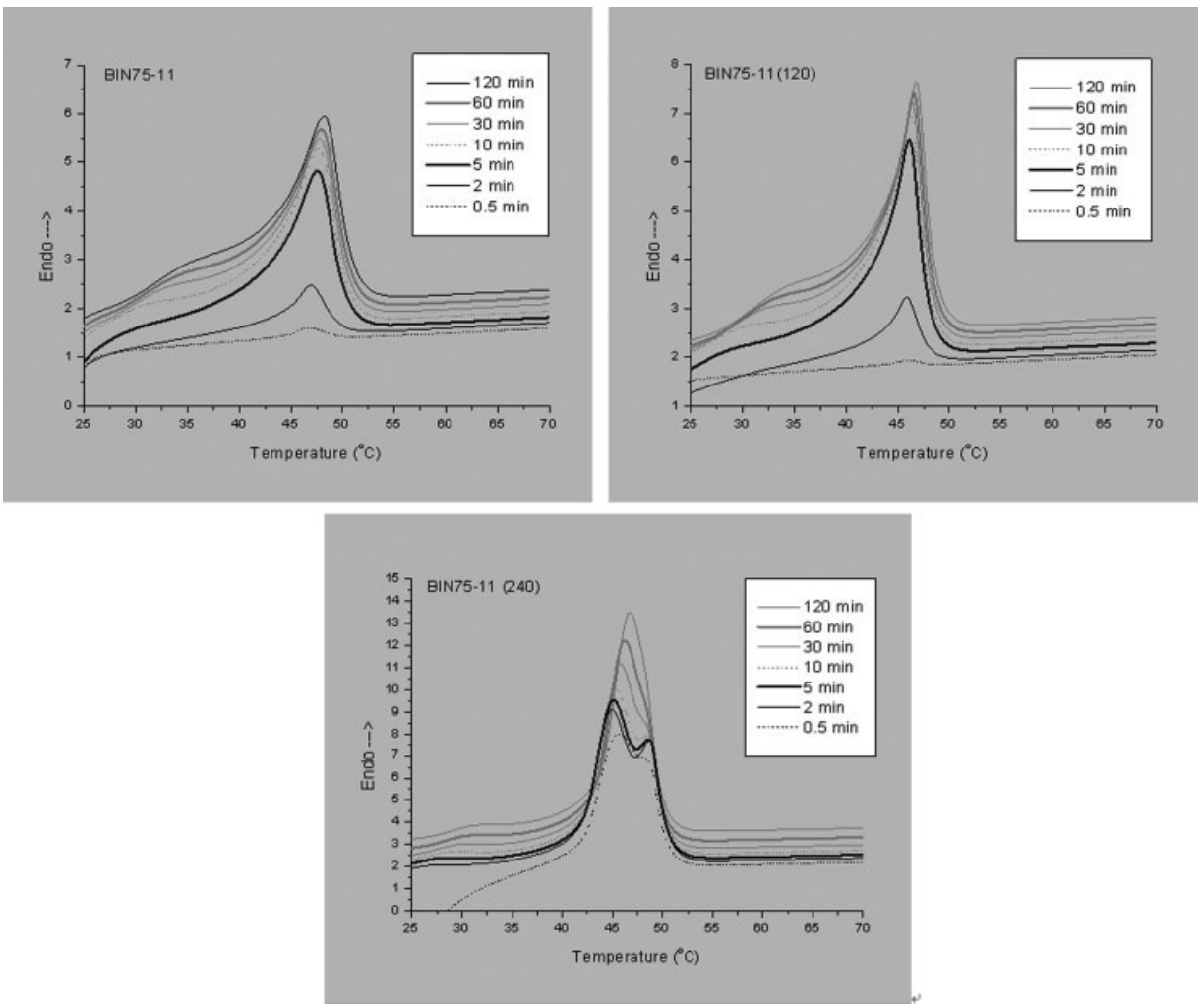

Figure 3 Heating scan after isothermal crystallization at 20°C for various times [during the first heating to remove the thermal history, the maximum temperature was 70°C for BIN75-11, 120°C for BIN75-11(120), and 240°C for BIN75-11(240)].

time needed to finish the isothermal crystallization, it can be observed that the higher T_c is, the lower the crystallization rate will be; the crystallization rate decreased with an increase in the BIN content in this series of SMPU ionomers, whether the neutralization agent was HAc or C8I. Also, the choice of the neutralization agent had some influence on the crystallization rate.

Theoretically, if eq. (3) can adequately follow the crystallization process, a plot of $\log\{-\ln[1 - X(t)]\}$ against $\log t$ should yield a straight line with slope n and intercept $\log K$. Double logarithmic plots of $\log\{-\ln[1 - X(t)]\}$ against $\log t$ for SMPU ionomers with various temperatures are shown in Figure 6. Each plot represents the linear dependence of $\log\{-\ln[1 - X(t)]\}$ against $\log t$, but with a slight deviation from the prediction when both parameters are large, indicating the existence of a secondary crystallization of PCL that occurs consecutively with the primary crystallization. The study of PCL (M_w = 80,000) by Kuo et al.[45] suggests that the PCL with a higher M_w value has the same tendency at a later stage in the crystallization process. The deviation can be attributed to the secondary crystallization involving fibrillar growth between the primary lamellae of the spherulite and leading to the occurrence of spherulite impingement.

The values of n and K for a particular sample can be determined from the initial linear portions of the double logarithmic plots shown in Figure 6. The results for different samples are summarized in Table III. n of the control sample and SMPU ionomer at 16–28°C in our experiment was around 2.0 and presented a slightly increasing trend with increasing temperature. This was a manifestation of the similar crystallization mechanisms in the control sample and SMPU ionomers with various ionic group contents quenched from 70°C.

The half-crystallization time [$t(0.5)$] is defined as the time at which the crystallinity is equal to 50%. It is related to Avrami parameter K and can be determined with the following expression:

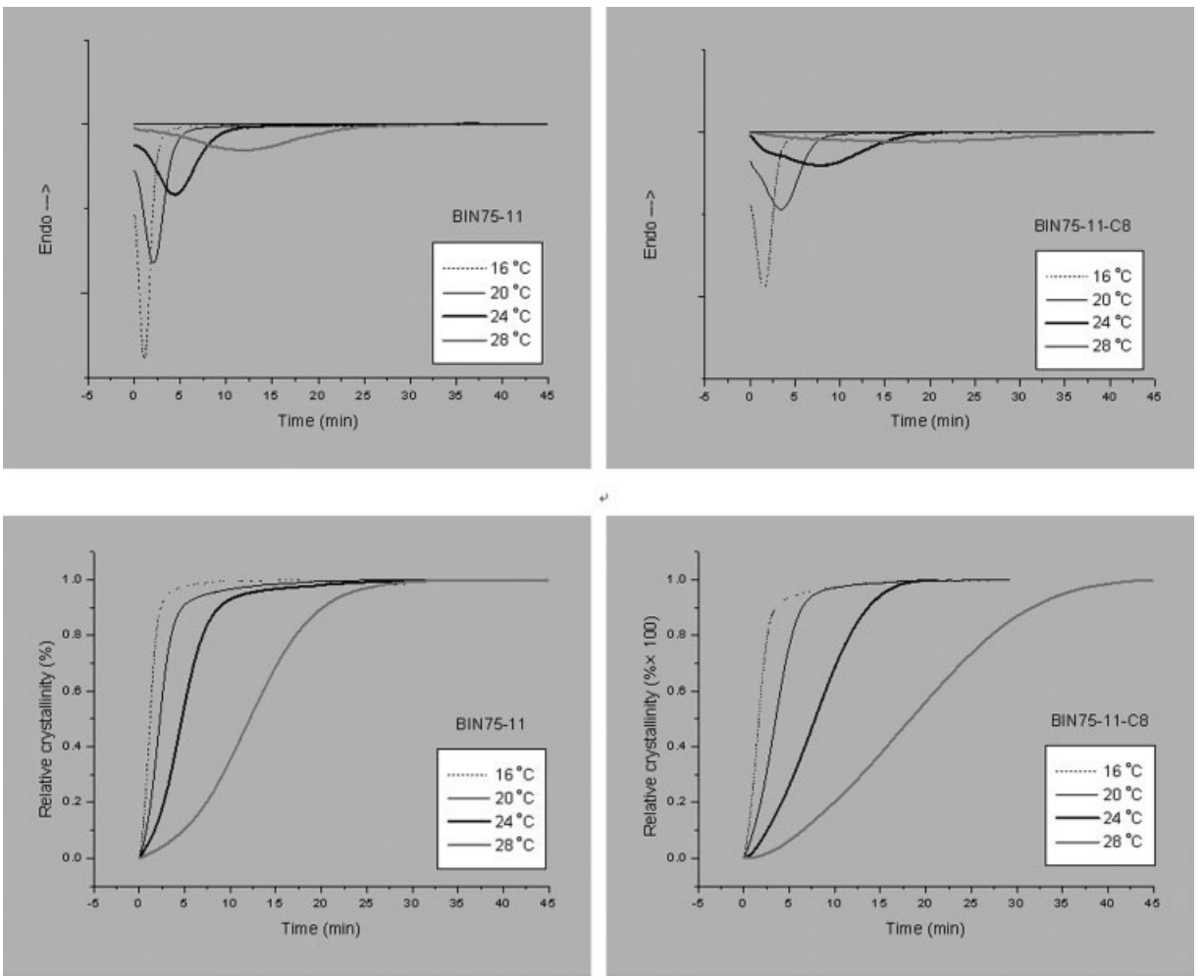

Figure 4 Development of the exothermic curve and relative crystallinity with time for isothermal crystallization.

$$K = \ln 2/[t(0.5)]^n \quad (4)$$

Table III summarizes the Avrami parameters for the soft segments of the PU ionomers. K, calculated from eq. (4), agrees well with that obtained experimentally and shown in Figure 6. It suggests that the Avrami equation analysis is adequate for describing the crystallization mechanism of this series of SMPU ionomers.[46]

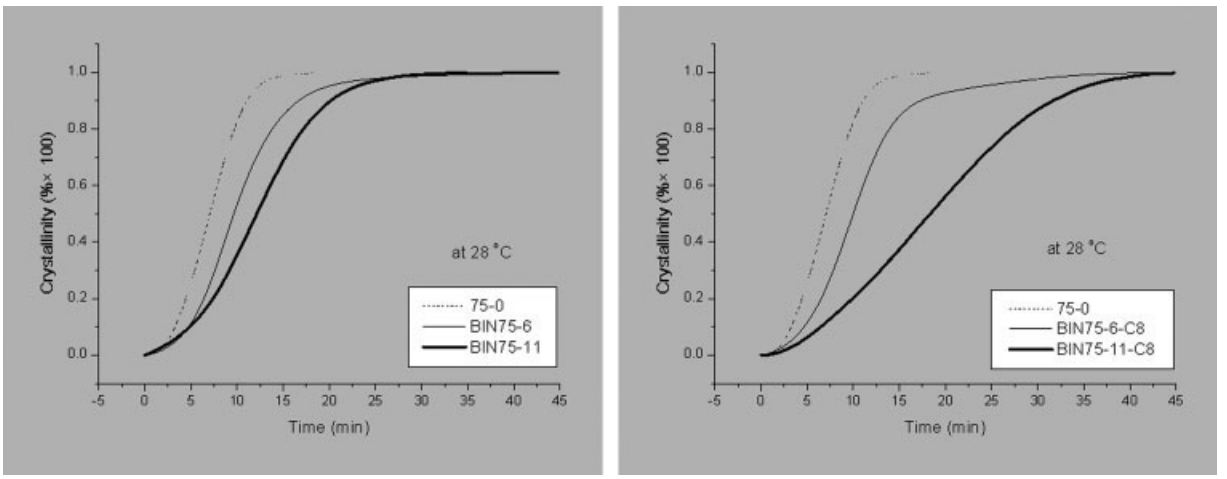

Figure 5 Development of the relative crystallinity with various ionic group contents for isothermal crystallization at 28°C.

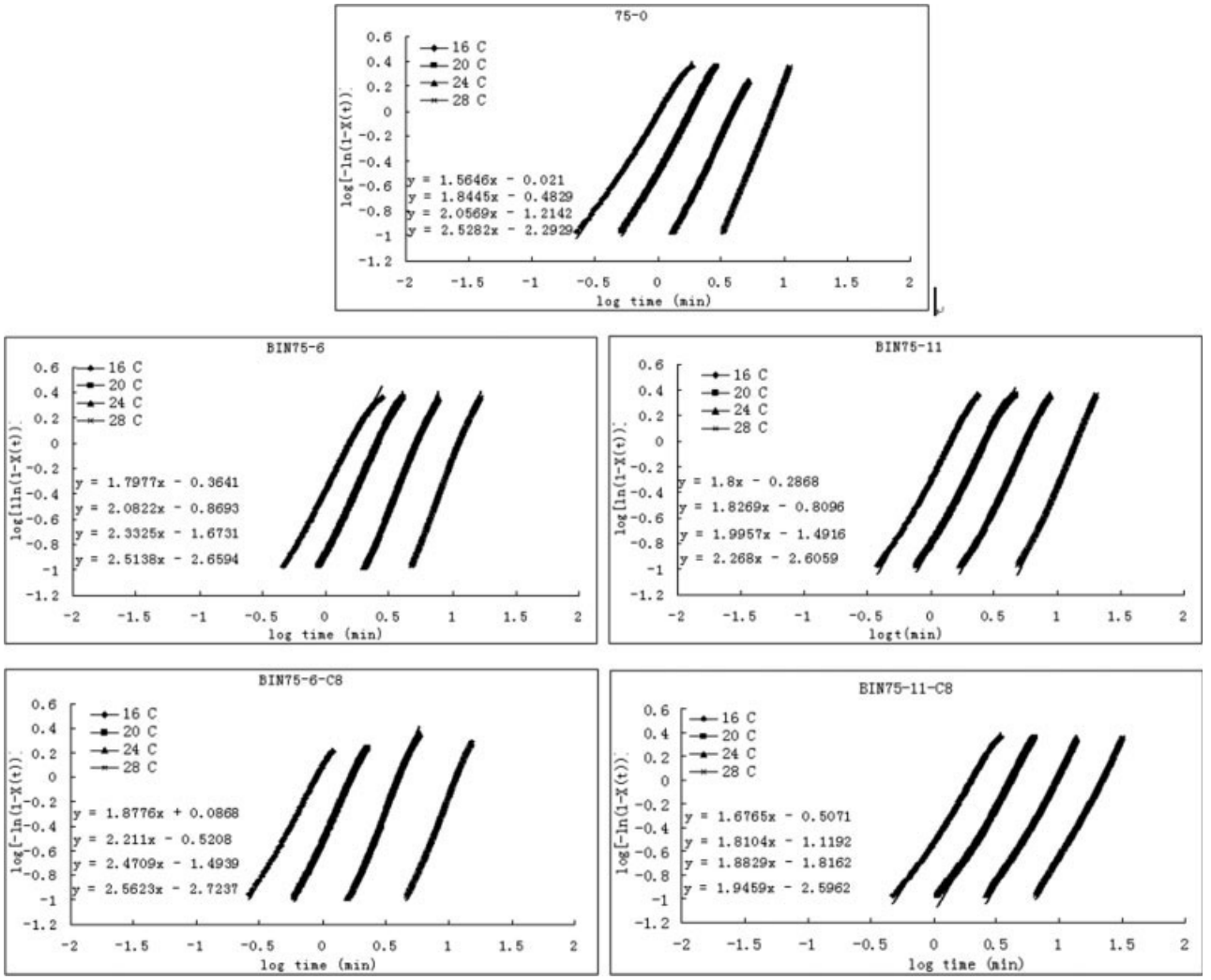

Figure 6 Plots of $\log\{-\ln[1 - X(t)]\}$ versus $\log t$ for isothermal crystallization at the indicated temperatures.

Usually, the rate of crystallization is mathematically defined as the inverse of $t(0.5)$. The values of $t(0.5)$ for different samples are summarized in Table III. It illustrates the fact that the crystallization rate decreased significantly with the introduction of the asymmetrical chain extender BIN. The greater the BIN weight content was, the lower the crystallization rate was, whether the neutralization agent was HAc or C8I. In a comparison of BIN75-11 and BIN75-11-C8, we found that the crystallization rate was much higher for the former specimen; this can be judged from the lower $t(0.5)$ value for BIN75-11.

An understanding of the BIN weight percentage dependence of Avrami parameter K is slightly more involved. Just as in the previous study reported by Chen et al.,[27] the incorporation of an ionic component into hard segments can disrupt the order of the hard segments, although increased cohesion among ionic groups does exist in some specific cases. Therefore, the insertion of ionic groups into hard segments can change the extent of phase mixing and subsequently influence the crystallization of the crystalline soft segment through the variation of the order of the hard domain. Therefore, in the isothermal crystallization testing routine (cooling from 70°C to room temperature, i.e., 20°C), the presence of BIN ionic groups slows the crystallization process significantly, although the crystallization mechanism does not obviously change. From a practical viewpoint, it is supposed to have a huge influence on the shape-memory function under specific programming conditions in this kind of SMPU ionomer, and this relation between the structure and properties will be further studied in our future work.

Equilibrium melting temperature (T_e)

A dominant sharp exothermic peak in the reheating DSC thermogram of our samples is considered to be the primary T_m. Figure 7 clearly reveals that T_m increased linearly with T_c. The experimental data can be fitted well by the Hoffman–Weeks equation:[47]

TABLE III
Parameters of Isothermal Crystallization

Sample	Temperature (°C)	Temperature (K)	n	log K	K	E (kJ/mol)	$t(0.5)$ (min)	$K = \ln 2/[t(0.5)]^n$	log K	T_e	T_m	Φ
75-0	16	289.15	1.56	−0.021	9.53×10^{-1}	54.36	0.831	9.25×10^{-1}	−0.034	54.1	45.77	0.23
	20	293.15	1.84	−0.483	3.29×10^{-1}		1.52	3.21×10^{-1}	−0.494		46.27	
	24	297.15	2.06	−1.214	6.11×10^{-2}		3.25	6.11×10^{-2}	−1.214		47.1	
	28	301.15	2.53	−2.293	5.09×10^{-3}		7.04	4.97×10^{-3}	−2.304		48.11	
BIN75-6	16	289.15	1.80	−0.364	4.33×10^{-1}	51.83	1.27	4.51×10^{-1}	−0.346	54.8	46.3	0.23
	20	293.15	2.08	−0.869	1.35×10^{-1}		2.17	1.38×10^{-1}	−0.860		46.79	
	24	297.15	2.33	−1.673	2.12×10^{-2}		4.38	2.21×10^{-2}	−1.656		47.63	
	28	301.15	2.51	−2.660	2.19×10^{-3}		9.66	2.32×10^{-3}	−2.635		48.63	
BIN75-11	16	289.15	1.80	−0.287	5.17×10^{-1}	59.11	1.2	4.99×10^{-1}	−0.302	52.9	46.11	0.19
	20	293.15	1.83	−0.810	1.55×10^{-1}		2.27	1.55×10^{-1}	−0.811		46.77	
	24	297.15	2.00	−1.492	3.22×10^{-2}		4.68	3.16×10^{-2}	−1.500		47.44	
	28	301.15	2.27	−2.606	2.48×10^{-3}		12.13	2.40×10^{-3}	−2.620		48.27	
BIN75-6-C8	16	289.15	1.88	0.087	1.22	66.87	0.74	1.22	0.087	54.2	47.46	0.19
	20	293.15	2.21	−0.520	3.02×10^{-1}		1.45	3.05×10^{-1}	−0.516		47.79	
	24	297.15	2.47	−1.494	3.21×10^{-2}		3.44	3.28×10^{-2}	−1.484		48.45	
	28	301.15	2.56	−2.724	1.89×10^{-3}		10	1.91×10^{-3}	−2.719		49.29	
BIN75-11-C8	16	289.15	1.68	−0.507	3.11×10^{-1}	62.26	1.64	3.02×10^{-1}	−0.519	54.1	46.6	0.21
	20	293.15	1.81	−1.119	7.60×10^{-2}		3.5	7.18×10^{-2}	−1.144		46.93	
	24	297.15	1.88	−1.816	1.53×10^{-2}		7.83	1.44×10^{-2}	−1.842		47.78	
	28	301.15	1.95	−2.596	2.53×10^{-3}		18.35	2.41×10^{-3}	−2.618		48.61	

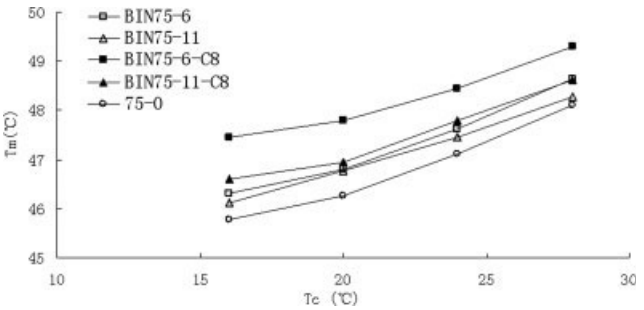

Figure 7 Plots of the observed values of T_m versus T_c for the SMPU ionomers.

$$T_m = \Phi T_c + (1 - \Phi)T_e \tag{5}$$

where $\Phi = 1/\gamma$ is the stability parameter depending on the crystal thickness (γ is the ratio of the lamellar thickness to the lamellar thickness of the critical nucleus at T_c). Φ in eq. (5) can have values between 0 and 1 (Φ = 0 and $T_m = T_e$, whereas Φ = 1 and $T_m = T_c$). The crystals are most stable for Φ = 0 and unstable for Φ = 1. T_e can be calculated from the intersection point between plots of T_m versus T_c and lines of $T_m = T_c$.

As shown in Figure 7, T_m for SMPU ionomers increased with T_c, as expected. The extrapolation of the observed T_m values to the line $T_m = T_c$ has been widely employed to calculate the T_e values of different copolymers and homopolymers.[48] However, in studies of segmented poly(ester urethane)s based on PCL by Bogdanow et al.[22] and linear polyethylenes and random copolymers at a low level of crystallinity by Alamo and coworkers,[49,50] this extrapolation method failed to describe the relations between T_m and T_c. Bogdanow et al. used different approaches to understand this scenario. First, the nonisothermal crystallization during cooling to a certain value of T_c causes the corresponding value of T_m to increase. Second, the observed dependence also arises from annealing during the heating scan, which causes the improvement in the crystal quality, and so T_m increases; the effect is particularly pronounced when T_c is lower. Therefore, in our investigation of T_e of SMPU ionomers, T_e was calculated from the T_c range above 20°C.

Table III summarizes the values of T_e of all the PU samples. The T_e values of the SMPU ionomer samples were quite similar to that of the control sample (75-0). After the introduction of ionic groups into the hard segment, Φ varied from 0.19 to 0.23 in the SMPU ionomer samples, and this suggested that the formation of crystals in the SMPU ionomer samples was rather stable. The Φ values of the PU ionomer samples were generally smaller than those of the control sample, 75-0, providing evidence that the

ionic groups in the hard segments improved the stability of the crystallization in the soft segment.

CONCLUSIONS

An investigation of the isothermal crystallization kinetics of SMPU ionomers was carried out with DSC. With the use of the Avrami equation, the crystallization mechanism of SMPU ionomer and control samples was analyzed. The results suggested that the n values of the SMPU ionomer and control samples were all around 2.0. The difference was the crystallization rate parameter K. After the introduction of ionic groups into the hard segment by chain extension with BIN, the crystallization rate decreased significantly, and the greater the BIN weight percentage was in the hard segment, the lower the crystallization rate was. Moreover, the neutralization agents also had some influence on the crystallization rate. In the melting behavior study, it was revealed that the melting peak of the SMPU ionomer quenched from 70°Cor 120°C could be mostly attributed to the primary crystallization, but the SMPU ionomer quenched from 240°C showed a dual-melting peak depending strongly on the isothermal crystallization time.

References

1. Lendlein, A.; Kelch, S. Angew Chem Int Ed 2002, 41, 2034.
2. Lendlein, A.; Langer, R. Science 2002, 296, 1673.
3. Li, F. K.; Zhang, X.; Hou, J. N.; Xu, M.; Luo, X. L.; Ma, D. Z.; Kim, B. K. J Appl Polym Sci 1997, 64, 1511.
4. Kim, B. K.; Shin, Y. J.; Cho, S. M.; Jeong, H. M. J Polym Sci Part B: Polym Phys 2000, 38, 2652.
5. Jeong, H. M.; Lee, S. Y.; Kim, B. K. J Mater Sci 2000, 35, 1579.
6. Tobushi, H.; Hashimoto, T.; Ito, N.; Hayashi, S.; Yamada, E. J Intell Mater Syst Struct 1998, 9, 127.
7. Kim, B. K.; Lee, S. Y.; Lee, J. S.; Baek, S. H.; Choi, Y. J.; Lee, J. O.; Xu, M. Polymer 1998, 39, 2803.
8. Tobushi, H.; Hara, H.; Yamada, E.; Hayashi, S. Smart Mater Struct 1996, 5, 483.
9. Kim, B. K.; Lee, S. Y.; Xu, M. Polymer 1996, 37, 5781.
10. Hayashi, S.; Ishikawa, N. J Coat Fabrics 1993, 23, 74.
11. Hu, J. L.; Zeng, Y. M.; Yan, H. J. Text Res J 2003, 73, 172.
12. Hu, J. L.; Yang, Z. H.; Yeung, L. Y.; Ji, F. L.; Liu, Y. Q. Polym Int 2005, 54, 854.
13. Hu, J. L.; Ji, F. L.; Wong, Y. W. Polym Int 2005, 54, 600.
14. Zhu, Y.; Hu, J. L.; Yeung, K. W.; Fan, H. J.; Liu, Y. Q. Chin J Polym Sci 2006, 24, 173.
15. Zhu, Y.; Hu, J. L.; Yeung, L. Y.; Liu, Y.; Ji, F. L.; Yeung, K. W. Smart Mater Struct 2006, 15, 1385.
16. Huang, W. M.; Yang, B.; An, L.; Li, C.; Chan, Y. S. Appl Phys Lett 2005, 86, 114105–114101.
17. Cho, J. W.; Kim, J. W.; Jung, Y. C.; Goo, N. S. Macromol Rapid Commun 2005, 26, 412.
18. Chen, S. J.; Su, J. C.; Zhao, W. B.; Liu, P. S. Polym Mater Sci Eng 2005, 21, 166.
19. Cha, D. I.; Kim, H. Y.; Lee, K. H.; June, Y. C.; Cho, J. W.; Chun, B. C. J Appl Polym Sci 2005, 96, 460.
20. Li, F. K.; Zhang, X.; Hou, J. A.; Zhu, W.; Xu, M. Acta Polym Sinica 1996, 4, 462.
21. Hou, J. A.; Ma, X. Q.; Luo, X. L.; Ma, D. Z.; Zhang, X.; Zhu, W.; Xu, M. In The International Symposium on Polymer Alloys and Composites; Choy, C. L.; Shin, F. G., Eds.; Hong Kong Polytechnic University: Hong Kong, 1992; p 211.
22. Bogdanow, B.; Toncheva, V.; Schacht, E.; Finelli, L.; Sarti, B.; Scandola, M. Polymer 1999, 40, 3171.
23. Jeong, H. M.; Ahn, B. K.; Cho, S. M.; Kim, B. K. J Polym Sci Part B: Polym Phys 2000, 38, 3009.
24. Jeong, H. M.; Ahn, B. K.; Kim, B. K. Polym Int 2000, 49, 1714.
25. Yang, J.-E.; Kong, J.-S.; Park, S.-W.; Lee, D.-J.; Kim, H.-D. J Appl Polym Sci 2002, 86, 2375.
26. Wei, X.; Yu, X. H. J Polym Sci Part B: Polym Phys 1997, 35, 225.
27. Chen, S. A.; Chan, W. C. J Polym Sci Part B: Polym Phys 1990, 28, 1499.
28. Grapski, J. A.; Cooper, S. L. Biomaterials 2001, 22, 2239.
29. Zhu, Y.; Hu, J. L.; Yeung, K. W.; Choi, K. F.; Liu, Y. Q.; Liem, H. M. J Appl Polym Sci 2007, 103, 545.
30. Brunette, C. M.; Hsu, S. L.; MacKnight, W. J. Macromolecules 1982, 15, 71.
31. Li, F. K.; Hou, J. A.; Zhu, W.; Zhang, X.; Xu, M.; Luo, X. L.; Ma, D. Z.; Kim, B. K. J Appl Polym Sci 1996, 62, 631.
32. Bogart, J. W. C. V.; Gibson, P. E.; Cooper, S. L. J Polym Sci Part B: Polym Phys 1983, 21, 65.
33. Crescenzi, V.; Manzini, G.; Calzolari, G.; Borri, C. Eur Polym J 1972, 8, 449.
34. Guo, Q.; Groeninckx, G. Polymer 2001, 42, 8647.
35. Defieuw, G.; Groeninckx, G.; Reynaers, H. Polymer 1989, 30, 595.
36. Defieuw, G.; Groeninckx, G.; Reynaers, H. Polymer 1989, 30, 2164.
37. Rim, P. B.; Runt, J. P. Macromolecules 1983, 16, 762.
38. Avrami, M. J Chem Phys 1939, 7, 1103.
39. Liu, S.; Yu, Y.; Cui, Y.; Zhang, H.; Mo, Z. J Appl Polym Sci 1998, 70, 2371.
40. Li, C.; Tian, G.; Zhang, Y.; Zhang, Y. Polym Test 2002, 21, 919.
41. Kim, S. H.; Ahn, S. H.; Hirai, T. Polymer 2003, 44, 5625.
42. Alwattari, A. A.; Lloyd, D. R. Polymer 1998, 39, 1129.
43. Lin, C. C. Polym Eng Sci 1983, 23, 113.
44. Cebe, P.; Hong, S.-D. Polymer 1986, 27, 1183.
45. Kuo, S. W.; Chan, S. C.; Chang, F. C. J Appl Polym Sci 2004, 42, 117.
46. Li, J.; Zhou, C. X.; Wang, G.; Tao, Y.; Liu, Q.; Li, Y. Polym Test 2002, 21, 583.
47. Hoffman, J. D.; Weeks, J. J. J Chem Phys 1962, 37, 1723.
48. Liu, Y.; Pan, C. Eur Polym J 1998, 34, 621.
49. Alamo, R. G.; Viers, B. D.; Mandelkern, L. Macromolecules 1995, 28, 3205.
50. Alamo, R. G.; Chan, E. K.M.; Mandelkern, L. Macromolecules 1992, 25, 6381.